

Citation for published version:

Redigueri, CF, de Jesus Andreoli Pinto, T, Bou-Chacra, NA, Galante, R, Lima Barros de Araújo, G, do Nascimento Pedrosa, T, Maria-Engler, SS, De Bank, PA 2016, 'Ozone gas as a benign sterilization treatment for PLGA nanofibre scaffolds', *Tissue Engineering part C Methods*, vol. 22, no. 4, pp. 338-347.
<https://doi.org/10.1089/ten.TEC.2015.0298>

DOI:

[10.1089/ten.TEC.2015.0298](https://doi.org/10.1089/ten.TEC.2015.0298)

Publication date:

2016

Document Version

Peer reviewed version

[Link to publication](#)

University of Bath

Alternative formats

If you require this document in an alternative format, please contact:
openaccess@bath.ac.uk

General rights

Copyright and moral rights for the publications made accessible in the public portal are retained by the authors and/or other copyright owners and it is a condition of accessing publications that users recognise and abide by the legal requirements associated with these rights.

Take down policy

If you believe that this document breaches copyright please contact us providing details, and we will remove access to the work immediately and investigate your claim.

**Final publication is available from Mary Ann Liebert, Inc.,
publishers <http://dx.doi.org/10.1089/ten.TEC.2015.0298>**

Ozone Gas as a Benign Sterilization Treatment for PLGA Nanofibre Scaffolds

Carolina Fracalossi Redigueri, MSc,^{1,2,*} Terezinha de Jesus Andreoli Pinto, PhD,¹ Nadia Araci Bou-Chacra, PhD,¹ Raquel Galante, MSc,^{1,3} Gabriel Lima Barros de Araújo, PhD,¹ Tatiana do Nascimento Pedrosa, MSc⁴, Silvy Maria-Engler, PhD⁴, and Paul A. De Bank, PhD^{5,**}

¹Departamento de Farmácia, Faculdade de Ciências Farmacêuticas, Universidade de São Paulo, Av. Prof. Lineu Prestes, 580–B13, Cidade Universitária, CEP 05508-000, São Paulo-SP, Brasil.

²Agência Nacional de Vigilância Sanitária, SIA Trecho 5, Área Especial 57, CEP 71205-050, Brasília-DF, Brasil.

³Centro de Química Estrutural, Instituto Superior Técnico, Universidade de Lisboa, Avenida Rovisco Pais 1, 1049-001 Lisboa, Portugal.

⁴Departamento de Análises Clínicas e Toxicológicas, Faculdade de Ciências Farmacêuticas, Universidade de São Paulo, Av. Prof. Lineu Prestes, 580–B17, Cidade Universitária, CEP 05508-000, São Paulo-SP, Brasil.

⁵Department of Pharmacy & Pharmacology and Centre for Regenerative Medicine, University of Bath, Bath, BA2 7AY, U.K.

* Corresponding author: Email address carolina.redigueri@usp.br, telephone +55 11 983 159 559

** Corresponding author: Department of Pharmacy & Pharmacology and Centre for Regenerative Medicine, University of Bath, Bath, BA2 7AY, U.K. Email address p.debank@bath.ac.uk, telephone +44 01225 384017.

Abstract

The use of electrospun nanofibres for tissue engineering and regenerative medicine applications is a growing trend as they provide improved support for cell proliferation and survival due, in part, to their morphology mimicking that of the extracellular matrix. Sterilization is a critical step in the fabrication process of implantable biomaterial scaffolds for clinical use, but many of the existing methods employed to date can negatively affect scaffold properties and performance. Poly(lactic-co-glycolic acid) (PLGA) has been widely used as a biodegradable polymer for 3D scaffolds, and can be significantly affected by current sterilization techniques. The aim of this study was to investigate pulsed ozone gas as an alternative method for sterilizing PLGA nanofibres. The morphology, mechanical properties, physicochemical properties, and response of cells to PLGA nanofibre scaffolds were assessed following different degrees of ozone gas sterilization. This treatment killed *Geobacillus stearothermophilus* spores, the most common biological indicator used for validation of sterilization processes. In addition, the method preserved all of the characteristics of non-sterilized PLGA nanofibres at all degrees of sterilization tested. These findings suggest that ozone gas can be applied as an alternative method for sterilizing electrospun PLGA nanofibre scaffolds without detrimental effects.

Keywords

Sterilization; Nanofibres; PLGA; Tissue Engineering; Regenerative Medicine; Ozone

Introduction

The use of electrospun nanofibres for tissue engineering is a growing trend; their structure mimics the natural fibres present in the extracellular matrix and has been shown to provide appropriate cues for cell proliferation, differentiation and survival (1-3). Numerous cell types, including mesenchymal stem cells, keratinocytes and hepatocytes, have shown superior cell viability on electrospun scaffolds in comparison to other scaffolds types (4,5), and

electrospun fibres have been demonstrated to have great potential in engineering a wide range of tissues (6-13). What is more, electrospinning is a cost-efficient technique for fabrication of micro- or nanofibres, either at laboratory or industrial scale (14), allowing efficient scale-up for clinical applications.

For clinical translation, implantable medical devices must be sterile, i.e. free from viable microorganisms (15). According to regulatory bodies for medical products, aseptic sterile manufacturing processes can be employed only when terminal sterilization process is not feasible (16,17). For electrospun scaffolds, this means that they should ideally be sterilized before *in vitro* cell seeding or, if used as a cell-free device, prior to implantation into a patient. As the nanostructural, mechanical, and physicochemical properties of electrospun fibres are critical to the cell-scaffold interaction and cell function, it is important that these features are unaffected by the sterilization procedure used.

Biomaterial scaffolds can be sterilized by physical methods (dry or wet heat, and irradiation) or chemical treatments, such as hypochlorite solution, aqueous ethanol, hydrogen peroxide vapour, and ethylene oxide gas (18,19). A number of these methods have been applied to polymer nanofibre scaffolds, resulting in a range of detrimental effects, including affecting scaffold morphology, polymer molecular weight, mechanical properties or degradation profiles (20-25). Hence, it is important to identify alternative methods of sterilization that do not affect the properties of polymer nanofibres. Ozone gas has an excellent sterilization capacity against a variety of microorganisms (26), and is attractive due to its low cost, use of natural inputs (oxygen), and applicability to thermosensitive materials (27). It has been used to treat food, water and sewage, to sterilize water bottles, polymeric or stainless steel medical devices, and to decontaminate hospital rooms (28). Although ozone is used primarily for disinfection, it has also been employed to intentionally introduce oxygen-containing functional groups on the surface of polymer scaffolds to increase wettability, an effect which can improve cell-material interactions (29-35). However, to date, its ability to efficiently sterilize polymer nanofibres has not been investigated.

Poly(lactic-co-glycolic acid) (PLGA) has been widely used as a biomaterial in recent decades (36). Because of its established biocompatibility, adjustable biodegradability and mechanical properties (7), it is perhaps the most widely used synthetic polymer for 3D scaffolds (37), and has been used to engineer many tissue types, including cartilage, bone, liver, nerve, skin, and blood vessels (38). It has also been widely studied as a biomaterial for electrospun scaffolds (39-44), but is sensitive to a number of physical and chemical sterilants. Therefore, using PLGA as a model polymer, the purpose of this study was to investigate the effects of a validated ozone gas sterilization method on electrospun PLGA nanofibre scaffolds by comparing scaffold morphology, mechanical properties, physicochemical properties, and cell response following different degrees of sterilization.

Materials and Methods

Materials

Poly(lactic-co-glycolic acid) (PLGA; Resomer® RG 756S, molecular weight 76-116 kDa) was purchased from Boehringer Ingelheim Ltd., UK, and 2,2,2-trifluoroethanol (TFE) from Alfa Aesar, UK. Biological indicator *Geobacillus stearothermophilus* (Attest™ 1262) was supplied by 3M, Brazil and the surgical paper by Cipamed Ltd., Brazil. Tryptone Soya Broth (TSB) was purchased from Difco Laboratories, UK, Fluid Thioglycollate Medium (FTM) from Oxoid Microbiology Products, UK. NIH 3T3 fibroblasts (#93061524) were acquired from Health Protection Agency, UK. All other materials were purchased from Sigma Aldrich, UK.

Scaffold fabrication

PLGA was dissolved to a concentration of 25% (w/v) in TFE by stirring for 24 hours at 20 °C. The polymer solution was transferred to a 10 mL glass syringe (Hamilton) and electrospun at 15 kV (73030P high voltage power supply, Genvolt, UK) through a 20G stainless steel needle towards a 15 x 15 cm grounded, aluminium foil-covered collector at a distance of 15 cm from the tip of the needle. A flow rate of 1.5 mL/h was maintained using a syringe

infusion pump (Cole Parmer, UK) and a total of 1 g PLGA deposited per mat. Three nanofibre mats were independently fabricated for each sterilization condition, with three matched non-sterilized controls per experiment.

Scaffold sterilization

A validated ozone gas sterilization procedure for medical devices (in accordance with ISO 14937 (45)) was used to sterilize the electrospun PLGA scaffolds. A prototype sterilization chamber (supplied by Ortosintese, São Paulo, Brazil) was used to apply ozone gas through the samples in a pulsed form. Each pulse was composed of four stages: vacuum, chamber filling, plateau (20 minutes), and vacuum. The humidity inside the chamber was up to 95%, with positive internal pressure ranging from 0.4 to 0.8 kgf/cm² during chamber filling and negative internal pressure ranging from -0.8 to -0.4 kgf/cm² during vacuum. Scaffolds were enclosed in surgical paper and exposed to either zero, two, four or eight pulses of ozonation.

Sterility assessment

To confirm that the ozone gas penetrated and sterilized the PLGA nanofibres, spore strips of the biological indicator *Geobacillus stearothermophilus* were wrapped into the scaffolds, enclosed in surgical paper and placed inside the sterilization chamber within plastic sleeves. Five indicator units were used for each sterilization condition. After two, four or eight pulses of ozonation, the biological indicators were incubated for 48 hours at 56 °C. Subsequently, the scaffolds from this experiment were aseptically cut into two pieces, placed in TSB or FTM, and incubated at 22.5 ± 2.5 °C and 32.5 ± 2.5 °C, respectively, for 14 days.

Field emission scanning electron microscopy (FE-SEM)

The morphology of sterilized and non-sterilized PLGA nanofibre scaffolds was examined by FE-SEM (FESEM6301F, JEOL) at an accelerating voltage of 5 kV. Prior to FE-SEM analysis,

specimens were sputter-coated (Quorum Q150T S) with a 10 nm layer of chromium to produce a conductive surface. Three samples of each scaffold were analysed, and three images were obtained from each sample. Mean fibre diameters were determined by randomly selecting 20 fibres from the central area of each picture, and measuring their diameters using ImageJ software (National Institutes of Health, Bethesda, MD; <http://rsb.info.nih.gov/ij/>).

Fourier transform-infrared spectroscopy (FTIR)

Fourier transform infrared spectroscopy (FTIR) was used to assess changes in the surface chemistry of the PLGA scaffolds. FTIR spectra were obtained using an FTIR spectrometer (PerkinElmer Spectrum 100) with an Attenuated Total Reflectance (ATR) accessory. For each sample, 32 scans were performed over a wavelength range of 4,000-500 cm^{-1} at a resolution of 8 cm^{-1} .

Water contact angle

PLGA nanofibre scaffolds were cut into squares of 1 x 1 cm and placed on glass slides. A 5 μL droplet of distilled water was carefully deposited onto each specimen and, after 60 seconds, an image of each droplet was recorded using a USB digital microscope (Veho VMS-001). Water contact angles were determined using the drop_analysis plug-in for ImageJ (obtained from <http://bigwww.epfl.ch/demo/dropanalysis>). Three replicates were performed for each of the triplicate scaffolds.

Thermal analysis

Thermogravimetric analysis of the nanofibre scaffolds was conducted using a Q500 thermogravimetric analyzer (TA Instruments, USA). Samples (approximately 4 mg) were placed in platinum pans and heated to 500 $^{\circ}\text{C}$ at a rate of 10 $^{\circ}\text{C}/\text{min}$, under an argon gas atmosphere (100 mL/min flow rate). Thermal characteristics of the scaffolds were evaluated

using differential scanning calorimetry (DSC) (DSC Q2000, TA Instruments, USA). Samples (approximately 1 mg) were placed in covered aluminium pans and heated from 0 to 150 °C at a rate of 10 °C/min under an argon gas atmosphere (50 mL/min flow rate), followed by cooling to ambient temperature. The glass transition temperature (T_g) was determined from the second scan of this cooled sample under the same conditions and temperature range (i.e. after thermal treatment). Each of the triplicate scaffolds was tested.

Mechanical properties

Tensile strength and Young's Modulus of scaffolds were measured using a Universal Testing Instrument (Instron 5965). Samples were cut into 20 mm × 10 mm strips, fixed in cardboard frames and a uniaxial force applied at a rate of 2 mm/min using a 100 N load cell at room temperature. Three replicates were tested for each of the triplicate scaffolds.

Cell culture

NIH 3T3 fibroblasts were cultured in Dulbecco's Modified Eagle's Medium supplemented with foetal bovine serum (10% v/v), penicillin (100 U/mL), streptomycin (100 µg/mL) and amphotericin B (250 ng/mL) and maintained at 37 °C with 5% CO₂ in a humidified incubator.

Cell morphology on scaffolds

Nanofibre scaffolds were cut into 9 mm diameter discs, placed in CellCrown inserts (Scaffdex Ltd.) within 48-well plates, and incubated in culture medium for 24 hours. Subsequently, 50 µL of a 3T3 cell suspension was seeded on each scaffold at a density of 3,000 cells/disc. Cells were allowed to attach for 20 minutes in this small volume before a further 600 µL of medium was carefully added to each well. After either 24 hours or 15 days, cells were fixed for 2 hours at 37 °C in a solution of serum-free culture medium containing 2.5% w/v glutaraldehyde. Cells were then post-fixed in an aqueous solution of osmium tetroxide and potassium ferrocyanide (both 1% w/v) for 1 hour at room temperature.

Samples were then washed with ultrapure water (Milli-Q, Millipore) and freeze dried. Dried samples were sputter coated with gold (150B Sputter Coater, Edwards) and observed by FE-SEM (FESEM6301F, JEOL) at an acceleration voltage of 5 kV.

Cell proliferation on scaffolds

To assess the biocompatibility of the sterilized PLGA scaffolds, cell proliferation over time in culture was measured using a resazurin assay of cell metabolic activity. 3T3 fibroblasts were seeded on PLGA nanofibres within CellCrown inserts as described above. Cells from the same suspension were seeded on tissue culture plastic to act as a positive control, while scaffolds in culture medium without cells were used as a negative control. Cell proliferation on the scaffolds was measured by a resazurin assay at various time points. An aqueous stock solution of 0.15 mg/mL resazurin sodium salt in Dulbecco's phosphate-buffered saline (pH 7.4) was prepared and filter-sterilized. At each time point, the culture medium was removed from each well and replaced with fresh medium containing resazurin solution at a concentration of 10% v/v. Plates were returned to the culture incubator for 2.5 hours, after which the medium was removed and 100 μ L aliquots from each well then transferred to a black 96-well microplate. Fresh, resazurin-free medium was added to each well of the cell-containing plates and returned to the incubator until the next assay time point. The fluorescence of sampled media was measured on a fluorescence plate reader (Biotek Synergy HT) with an excitation wavelength of 540 nm and emission wavelength of 590 nm. The values obtained from negative control scaffolds were subtracted to determine the fluorescent signal originating from the cellular activity. Triplicate wells were assessed for each of the triplicate scaffolds and the mean \pm standard error fluorescence value at each time point determined from three independent experiments.

Statistical analysis

All experiments were performed three times and data are reported as mean \pm standard error from of the three independent replicates. One-way analysis of variance, in conjunction with Tukey's *post hoc* test, was used to analyse differences between groups. A value of $p < 0.05$ was considered statistically significant.

Results

Effectiveness of sterilization method

Spores of *Geobacillus stearothermophilus* are a commonly used biological indicator and were employed in this study to determine the effectiveness of ozone gas treatment as a means of sterilizing PLGA nanofibres. Spore strips were wrapped inside PLGA scaffolds and, following pulsed ozone exposure, incubated for 48 hours at 56 °C. Sterilized and non-sterilized biological indicators showed different outcomes. As shown in Fig. 1, the control, non-sterilized indicator turned yellow following incubation, demonstrating bacterial growth. All of the sterilized indicators remained purple, confirming that the ozone gas was able to penetrate the pores of the nanofibre scaffolds and sterilize the enclosed biological indicator. After 14 days of incubation in TSB or FTM, all tubes containing the ozone-sterilized scaffolds remained clear, i.e., there was no growth of microorganisms inside the tubes, confirming that the nanofibre scaffolds were sterile after two, four, or eight pulses of ozonation.

Scaffold morphology

Any effects of ozone gas sterilization on the morphology of the PLGA nanofibres was assessed by FE-SEM. Fig. 2 shows micrographs of non-sterilized and ozone-sterilized nanofibres. All fibres were smooth and bead-free, with no observable differences between the groups, no signs of damage to any of the scaffolds, and no changes in the mean nanofibre diameter (Table 1).

Surface characterization

Attenuated Total Reflectance Fourier Transform Infrared Spectroscopy (ATR-FTIR) was used to explore the surface chemistry of the sterilized and non-sterilized PLGA scaffolds (Fig. 3). The spectra show typical peaks of ester carbonyl groups ($\sim 1,747\text{ cm}^{-1}$), attributable to C=O stretching, and peaks between 1,200 to 1,050 cm^{-1} , which correspond with C-O-C stretching (46). The spectra of the scaffolds treated with two, four, and eight pulses of ozone gas were very similar to the spectra of non-sterilized nanofibres, with no visible appearance of additional peaks following ozone treatment. The values of water contact angle of non-sterilized and sterilized scaffolds are also presented in Table 1. Sterilized scaffolds exhibited lower contact angles in comparison to the non-sterilized group. Despite slight decreases in contact angles when increasing the number of ozone treatment pulses, there were no significant difference between the groups ($p > 0.05$).

Thermal characterization

The thermogravimetric and DSC curves of the sterilized and non-sterilized PLGA scaffolds are shown in Fig. 4, and the thermal properties of the scaffolds are summarized in Table 1. The thermogravimetric curves (Fig. 4A) indicate that the thermal decomposition processes of all samples were similar and occurred in a single step, ranging from approximately 280 to 500 °C, with a weight loss of more than 97%. Thermogravimetric analysis of PLGA nanofibres has been previously performed and similar results were reported (47). DSC curves of PLGA scaffolds showed a weak endothermic event in the range of 50-65 °C (Fig. 4B). Since no weight loss was seen in thermogravimetric curves in this region, the event can be assigned to a typical enthalpic relaxation superimposed on glass transition (T_g) characteristic of PLGA materials (48-50), which is evidence of amorphicity. The glass transitions temperatures were clearly determined after removing the previous thermal history by thermal treatment of the samples (Fig. 4C; Table 1).

Mechanical properties

The values of tensile strength and Young's Modulus of non-sterilized and sterilized scaffolds are shown in Table 1. Ozone gas treatment of up to four pulses did not significantly affect the mechanical properties of the scaffolds ($p > 0.05$). However, eight pulses of ozone gas resulted in a decrease in the Young's Modulus of the PLGA scaffolds when compared to the non-sterilized group ($p < 0.05$). Both tensile strength and Young's Modulus of scaffolds sterilized by eight pulses were significantly lower when compared to the scaffolds sterilized by two pulses ($p < 0.05$ and $p < 0.01$, respectively).

Cell behaviour

To ascertain the effect of ozone gas sterilization on the biocompatibility of PLGA nanofibre scaffolds, 3T3 fibroblasts were seeded as a model cell. Cell morphology was examined by FE-SEM, and cell proliferation determined by resazurin reduction assays. FE-SEM images of cell morphology on non-treated and ozone-treated PLGA scaffolds at 24 hours and 15 days post seeding are presented in Fig. 5 and Fig. 6, respectively. After 24 hours cells had adhered and spread well on all scaffolds, with clear evidence of infiltration into scaffold pores and intimate interaction of cells with individual nanofibres (Fig. 5). After 15 days, cells existed in confluent layers on all scaffolds, and no apparent differences in cell morphology were observed on treated or non-treated scaffolds at either time point (Fig. 6).

To investigate whether ozone sterilization affected cell proliferation on PLGA nanofibres, 3T3 fibroblasts growth was studied over a period of 14 days (Fig. 7). Although there appeared to be a marginal reduction in proliferation on ozone-treated scaffolds in comparison to non-sterilized ones at all time points, these differences were not statistically significant.

Discussion

A critical step in the fabrication of any implantable medical device is sterilization. Although there are many sterilization methods, each device has its own critical parameters that must be conserved to maintain its efficacy and safety. A number of approaches have been examined for the sterilization of scaffolds for tissue engineering applications. However, most result in modification of one or more of a scaffold's morphological, mechanical or physicochemical properties. This study examined pulsed ozone gas sterilization as an alternative approach, with the aim of preserving scaffold properties post-sterilization. Nanofibrous matrices are particularly susceptible to modification during sterilization, so we tested the applicability of this technique against this type of scaffold. PLGA was chosen as the scaffold material due to its widespread use in tissue engineering applications and consequent potential for clinical translation. Of the possible compositions of PLGA, 75:25 (lactide:glycolide) was selected as it provided the most comparable scaffold to those used in previous investigations into the effects of sterilization techniques on PLGA nanofibres (22,24,25,51,52).

G. stearothermophilus spores are a common indicator used in the validation of ozone sterilization methods, and have been shown to be the most resistant indicator to this kind of sterilization process (28,53). Importantly, this study demonstrates that when the biological indicator was wrapped within PLGA nanofibres and exposed to two, four or eight pulses of ozone gas, the spores were killed (Fig. 1), suggesting that this procedure offers efficient sterilization even at the lowest number of ozone pulses employed. Subsequent culture of ozone-treated nanofibres for 14 days in either Tryptone Soya Broth, commonly used to cultivate fungi and aerobic bacteria, or Fluid Thioglycollate Medium, primarily intended for the culture of anaerobic bacteria (54), confirmed the lack of viable bacteria or fungi in these scaffolds.

Following successful sterilization of PLGA nanofibres, we investigated whether ozone gas treatment affected scaffold morphology, physicochemical, thermal and mechanical properties, and cell-material interactions. Scanning electron microscopy (SEM)

analysis demonstrated that scaffold morphology was unaffected by ozone gas sterilization (Fig. 2), and the nanofibre diameters also remained unchanged (Table 1). These results are comparable to exposure of PLGA nanofibres to electron beam (25), gamma (51,52), and UV (22,24) irradiation, which have also been shown to have no effect on fibre morphology and diameter. Conversely, wet chemical treatments such as ethanol, peracetic acid or antimicrobial solution, have been shown to significantly decrease PLGA nanofibres diameters (22,51).

Effects of ozone gas treatment on the surface characteristics of the PLGA nanofibres were assessed by FTIR analysis and water contact angle measurement. ATR-FTIR spectroscopy showed that, in comparison to untreated controls, no additional functional groups were present on the sterilized scaffolds, and peak intensities were unaffected (Fig. 3). Depending on their chemical structure, polymer exposure to ozone gas has been shown to result in the generation of a number of functional groups, such as peroxides, hydroperoxides and carboxyls *via* oxidation mechanisms. While there are no literature examples of PLGA modification *via* ozone treatment, poly-L-lactic acid (PLLA), has been functionalized with cell-adhesive species *via* the groups generated by ozone gas exposure (34,35,55). In comparison, the lack of chemical modification observed in this study is most likely due to the different ozone treatment methods employed rather than differences in the polymers. In this study, the PLGA nanofibre samples were exposed to pulses of ozone at a relatively low pressure, with each pulse lasting ~40 minutes. This contrasts with continuous ozone flow in PLLA treatment, either in a dried chamber (35) or bubbled through isopropyl alcohol in a mixture with oxygen (34,55). Based on our results, pulsed ozone gas appears to be a milder method than continuous ozone flow in terms of polymer oxidation, while still possessing the ability to kill microbial contaminants.

Following ATR-FTIR analysis, we investigated the wettability of the PLGA nanofibres by measurement of water contact angle. Surface wettability is affected by the chemical characteristics of the surface, with hydrophilic surfaces having a greater wettability than hydrophobic ones. Indeed, cell scaffolds fabricated from hydrophobic polymers, including

PLGA, are often post-treated to confer greater wettability, with the general belief being that this improves cell adhesion and growth. Following ozone treatment of PLGA nanofibres, although there was a downward trend in the water contact angle with increasing ozone pulses, this decrease was not statistically significant (Table 1). As expected from the lack of apparent surface chemistry changes visible in ATR-FTIR spectra, this demonstrates that ozone gas treatment had no effect on PLGA nanofibre wettability.

While the gross morphology and surface properties of PLGA nanofibres were unaffected by pulsed ozone gas treatment, it was also important to assess whether or not the scaffolds' bulk properties were modified by this procedure. PLGA is an amorphous solid undergoing two major transitions, the glass transition (T_g) and enthalpy relaxation, both of which can be affected by sterilization procedures, and may result in changes to the mechanical properties of the material (56,57). Thermogravimetric analysis and differential scanning calorimetry of untreated and ozone-treated PLGA nanofibres demonstrated that all samples had very similar thermal profiles (Fig. 4), and the calculated values of both T_g and enthalpy relaxation were unaffected by the sterilization process (Table 1; $p>0.05$). Previous studies on the effect of electron beam radiation on PLGA revealed a decrease in molecular weight and concomitant decrease in T_g with increasing radiation dose (58,59). A similar relationship was observed when PLGA was exposed to gamma irradiation (56). The similarities in thermal characteristics between ozone treatments observed in this study suggest that there were no deleterious effects of ozone gas exposure on the bulk polymer within the scaffolds, i.e. no polymer chain scission.

These observations are confirmed, at least in part, by the analysis of tensile strength and Young's Modulus, important parameters which can be affected by sterilization, and impact on a scaffold's suitability within a particular biomechanical environment. In the present study, ozone gas sterilization preserved the mechanical properties of PLGA nanofibres following two and four pulses of ozone gas, with no significant differences between treated and non-treated groups (Table 1; $p>0.05$). However, eight pulses of ozone

gas significantly decreased the tensile strength of the nanofibres ($p < 0.05$), although only in comparison to two pulses, not the untreated control. Similarly, eight pulses of ozone resulted in a significantly reduced Young's Modulus compared to zero or two pulses (Table 1; $p < 0.05$). Irradiation-based sterilization methods penetrate polymer matrices and change their bulk properties. For example, the mechanical properties of PLGA nanofibres have been shown to be severely compromised by electron beam or UV irradiation (24,25) while, conversely, gamma irradiation has been shown to increase the Young's modulus and ultimate tensile strength of PLGA nanofibres, although the rate of *in vitro* degradation was accelerated following this treatment (52). Selim *et al*, compared PLGA nanofibre sterilization by gamma irradiation, ethanol or peracetic acid, and determined that all three methods reduced the tensile strength of the scaffolds, with ethanol treatment resulting in an especially weak and brittle matrix (51). Ozone gas sterilization is a surface phenomenon, with no expected penetration into the bulk structure of the fibres. However, the mechanical properties of scaffolds exposed to eight pulses of ozone gas suggest that some bulk modification of the polymer structure occurred, which was not detected by the other analytical techniques employed in this study. One possibility, although one that was not apparent during SEM analysis, is modification of fibre arrangement within the matrices, a phenomenon known to affect mechanical properties of nanofibre scaffolds (60,61). Nonetheless, while the effects of eight ozone pulses require further investigation, we demonstrate that, unlike other sterilization techniques, two and four pulses of ozone gas do not alter the morphology, physicochemical and bulk properties of PLGA nanofibres.

For a sterilization technique to be suitable for use in tissue engineering and regenerative medicine applications, the response of cells to the scaffold should ideally not be adversely affected. We employed 3T3 fibroblasts as a model cell line to examine morphology and proliferation on PLGA nanofibres following ozone sterilization. No apparent morphological differences were observed between untreated and ozone-treated scaffolds 24 hours after seeding (Fig. 5), with all cells well spread and demonstrating significant

interaction with the fibres, and infiltration into the matrices. Similarly, after 15 days, there were no differences between the appearance of the 3T3 cells on the untreated and ozone sterilized PLGA nanofibres (Fig. 6). The cells were confluent on all matrices with evidence of significant extracellular matrix deposition, although the SEM processing resulted in artificial cracks appearing due to dehydration of the cells and scaffolds. Interestingly, this enabled the observation of cells deeper within the scaffolds, with evidence that the fibroblasts had infiltrated the 3D structure of the nanofibres to generate a multi-layered structure (Fig. 6E-H). Proliferation on the nanofibres was assessed by monitoring the reduction of resazurin to resorufin over a period of 14 days to determine the relative metabolic activity of cells on the different scaffolds (Fig. 7). The increasing fluorescence over time clearly indicated a concomitant increase in the number of cells on all scaffolds, with no significant differences between untreated and ozone-treated scaffolds, or between the ozone-treated groups ($p > 0.05$). Other sterilization treatments have also been shown to result in unaltered cell responses to PLGA nanofibre scaffolds. For example, NIH 3T3 proliferation was unaffected by electron beam irradiation (25), and short wave UV irradiation had no effect on porcine smooth muscle cell proliferation (24). Other studies, although lacking proliferation data, also suggest that gamma irradiation does not affect cell response to PLGA nanofibres (51,52), while ethanol treatment has been shown to have varied effects. Selim *et al* demonstrated that a co-culture of fibroblasts and keratinocytes was unaffected by ethanol sterilization (51), while Braghirolli *et al* described a reduction in mesenchymal cell adhesion and spreading on ethanol-treated PLGA nanofibres (22). These methods, although not affecting cell response, do, however, affect other properties of PLGA nanofibres, such as morphology, fibre diameter and mechanical properties, as described above. Hence pulsed ozone gas treatment, unlike other sterilization techniques, offers the possibility of effective scaffold sterilization, while maintaining the as-fabricated design parameters of PLGA nanofibre scaffolds. As PLGA is susceptible to modification during sterilization but was unaffected by this method, it is likely that ozone gas treatment will be equally efficacious

with other polyesters, such as PLLA and polycaprolactone, as well as more resilient polymers in other chemical classes, and to other types of scaffold in addition to nanofibres.

In conclusion, we have demonstrated that pulsed ozone gas is an efficient sterilization method for PLGA nanofibre scaffolds, killing *G. stearothermophilus*, the most common biological indicator used for validation of ozone gas sterilization processes. Despite PLGA nanofibres being susceptible to modification and degradation during sterilization, this method preserved the as-fabricated properties of the scaffolds, including efficacy of cell adhesion and growth, a feat which other sterilization methods are unable to achieve. As such, pulsed ozone gas sterilization offers an inexpensive and effective means of ensuring the safety and performance of tissue engineering scaffolds for clinical applications.

Acknowledgments

The authors would like to thank the National Council of Technological and Scientific Development of Brazil (CNPq-248814/2013-3), the University of São Paulo, and the University of Bath Global Partner Research Scholarship Scheme for funding this research. We gratefully acknowledge Mrs Tais Cecchi (Brasil Ozônio) for the use of the ozone sterilizer, Mr William Capelupi (TA Instruments, São Paulo) for access to their laboratory facility in São Paulo, Mr Nick Waywell (Department of Mechanical Engineering, University of Bath) for advice on mechanical testing, and Dr Ursula Potter and Dr John Mitchels (Microscopy and Analysis Suite, University of Bath) for their help and advice with electron microscopy.

Disclosure Statement

No competing financial interests exist.

References

1. Lim, S.H., and Mao, H-Q. Electrospun scaffolds for stem cell engineering. *Adv Drug Deliv Rev* **61**, 1084, 2009.
2. Beachley, V., and Wen, X. Polymer nanofibrous structures: Fabrication, biofunctionalization, and cell interactions. *Prog Polym Sci* **35**, 868, 2010.
3. Kai, D., Jin, G., Prabhakaran, M.P., and Ramakrishna, S. Electrospun synthetic and natural nanofibers for regenerative medicine and stem cells. *Biotechnol J* **8**, 59, 2013.
4. Agarwal, S., Wendorff, J.H., and Greiner, A. Use of electrospinning technique for biomedical applications. *Polymer* **49**, 5603, 2008.
5. Yoo, H.S., Kim, T.G., and Park, T.G. Surface-functionalized electrospun nanofibers for tissue engineering and drug delivery. *Adv Drug Deliv Rev* **61**, 1033, 2009.
6. Bini, T.B., Gao, S., Wang, S., Lim, A., Hai, L.B., and Ramakrishna, S. Electrospun poly (L-lactide-co-glycolide) biodegradable polymer nanofibre tubes for peripheral nerve regeneration. *Nanotechnology* **15**, 1459, 2004.
7. Blackwood, K.A., McKean, R., Canton, I., Freeman, C.O., Franklin, K.L., Cole, D., *et al.* Development of biodegradable electrospun scaffolds for dermal replacement. *Biomaterials* **29**, 3091, 2008.
8. Choi, J.S., Lee, S.J., Christ, G.J., Atala, A., and Yoo, J.J. The influence of electrospun aligned poly(epsilon-caprolactone)/collagen nanofiber meshes on the formation of self-aligned skeletal muscle myotubes. *Biomaterials* **29**, 2899, 2008.
9. Thorvaldsson, A., Stenhamre, H., Gatenholm, P., and Walkenstrom, P. Electrospinning of highly porous scaffolds for cartilage regeneration. *Biomacromolecules* **9**, 1044, 2008.
10. Jia, L., Prabhakaran, M.P., Qin, X., and Ramakrishna, S. Stem cell differentiation on electrospun nanofibrous substrates for vascular tissue engineering. *Mater Sci Eng C Mater Biol Appl* **33**, 4640, 2013.

11. Yeatts, A.B., Both, S.K., Yang, W., Alghamdi, H.S., Yang, F., Fisher, J.P., *et al.* In Vivo Bone Regeneration Using Tubular Perfusion System Bioreactor Cultured Nanofibrous Scaffolds. *Tissue Eng Part A* **20**, 139, 2014.
12. Morris, G.E., Bridge, J.C., Brace, L.A., Knox, A.J., Aylott, J.W., Brightling, C.E., *et al.* A novel electrospun biphasic scaffold provides optimal three-dimensional topography for in vitro co-culture of airway epithelial and fibroblast cells. *Biofabrication* **6**, 035014, 2014.
13. Pulikkot, S., Greish, Y.E., Mourad, A-H.I., and Karam, S.M. Establishment of a three-dimensional culture system of gastric stem cells supporting mucous cell differentiation using microfibrous polycaprolactone scaffolds. *Cell Prolif* **47**, 553, 2014.
14. Ji, W., Sun, Y., Yang, F., van den Beucken, J.J.J.P., Fan, M., Chen, Z., *et al.* Bioactive electrospun scaffolds delivering growth factors and genes for tissue engineering applications. *Pharm Res* **28**, 1259, 2011.
15. European Commission. Council Directive 90/385/EEC on the approximation of the laws of the Member States relating to active implantable medical devices, *Official Journal L189*, 17, 1990.
16. World Health Organization. Expert Committee on Specifications for Pharmaceutical Preparations. Forty-fifth report. Geneva, Switzerland: World Health Organization (WHO Technical Report Series, No. 961), 2011. Available from URL: http://whqlibdoc.who.int/trs/who_trs_961_eng.pdf
17. US Food and Drug Administration. Guidance for Industry, Sterile Drug Products Produced by Aseptic Processing – Current Good Manufacturing Practice. Rockville, Maryland, USA: Food and Drug Administration, 2004. Available from URL: <http://www.fda.gov/downloads/Drugs/GuidanceComplianceRegulatoryInformation/Guidances/ucm070342.pdf>
18. Pinto, T.J.A., Kaneko, T.M., and Pinto, A.F. Controle biológico de qualidade de produtos farmacêuticos, correlatos e cosméticos, 3rd ed. São Paulo: Atheneu Editora, 2010.

19. US Pharmacopeial Convention, Inc. United States Pharmacopeia and National Formulary (USP 35-NF 30). Rockville, Maryland, USA: US Pharmacopeial Convention, Inc., 2012.
20. Andrews, K.D., Hunt, J.A., and Black, R.A. Effects of sterilisation method on surface topography and in-vitro cell behaviour of electrostatically spun scaffolds. *Biomaterials* **28**, 1014, 2007.
21. Bosworth, L.A., Gibb, A., and Downes, S. Gamma irradiation of electrospun poly(ϵ -caprolactone) fibers affects material properties but not cell response. *J Polym Sci Pol Phys* **50**, 870, 2012.
22. Braghirolli, D.I., Steffens, D., Quintiliano, K., Acasigua, G.A.X., Gamba, D., Fleck, R.A., *et al.* The effect of sterilization methods on electronspun poly(lactide-co-glycolide) and subsequent adhesion efficiency of mesenchymal stem cells. *J Biomed Mater Res* **102**, 700, 2014.
23. Dånmark, S., Finne-Wistrand, A., Schander, K., Hakkarainen, M., Arvidson, K., Mustafa, K., *et al.* In vitro and in vivo degradation profile of aliphatic polyesters subjected to electron beam sterilization. *Acta Biomater* **7**, 2035, 2011.
24. Yixiang, D., Yong, T., Liao, S., Chan, C.K., and Ramakrishna, S. Degradation of electrospun nanofiber scaffold by short wave length ultraviolet radiation treatment and its potential applications in tissue engineering. *Tissue Eng Part A* **14**, 1321, 2008.
25. Lee, J.B., Ko, Y.G., Cho, D., Park, W.H., and Kim, B.N. Modification of PLGA Nanofibrous Mats by Electron Beam Irradiation for Soft Tissue Regeneration. *J Nanomater* **2015**, Article ID 295807, 2015.
26. Gurley, B. Ozone: pharmaceutical sterilant of the future? *J Parenteral Sci Technol* **39**, 256, 1985.
27. Moat, J., Cargill, J., Shone, J., and Upton, M. Application of a novel decontamination process using gaseous ozone. *Can J Microbiol* **55**, 928, 2009.

28. Sousa, C.S., Torres, L.M., Azevedo, M.P.F., de Camargo, T.C., Graziano, K.U., Lacerda, R.A., *et al.* Sterilization with ozone in health care: an integrative literature review. *Rev Esc Enferm USP* **45**, 1243, 2011.
29. Bilgin, S., Isik, M., Yilgor, E., and Yilgor, I. Hydrophilization of silicone-urea copolymer surfaces by UV/ozone: Influence of PDMS molecular weight on surface oxidation and hydrophobic recovery. *Polymer* **54**, 6665, 2013.
30. Charpentier, P.A., Maguire, A., and Wan, W.K. Surface modification of polyester to produce a bacterial cellulose-based vascular prosthetic device. *Appl Surf Sci* **252**, 6360, 2006.
31. Kikkawa, Y., Fukuda, M., Ichikawa, N., Kashiwada, A., Matsuda, K., Kanetsato, M., *et al.* Tuning the enzymatic hydrolysis of biodegradable polyesters and its application to surface patterning. *J Mater Chem A* **1**, 4667, 2013.
32. Kwon, J.H., Kim, S.S., Kim, B.S., Sung, W.J., Lee, S.H., Lim, J.K., *et al.* Histological behavior of HDPE scaffolds fabricated by the “Press-and-Baking” method. *J Bioact Compat Pol* **20**, 361, 2005.
33. Mitchell, S.A., Poulsson, A.H.C., Davidson, M.R., Emmison, N., Shard A.G., and Bradley, R.H. Cellular attachment and spatial control of cells using micro-patterned ultra-violet/ozone treatment in serum enriched media. *Biomaterials* **25**, 4079, 2004.
34. Ho, M.H., Lee, J.J., Fan, S.C., Wang, D.M, Hou, L.T., Hsieh, H.J., *et al.* Efficient Modification on PLLA by Ozone Treatment for Biomedical Applications. *Macromol Biosci* **7**, 467, 2007.
35. Suh, H., Hwang, Y.S., Lee, J.E., Han, C.D., and Park, J.C. Behavior of osteoblasts on a type I atelocollagen grafted ozone oxidized poly L-lactic acid membrane. *Biomaterials* **22**, 219, 2001.
36. Yang, S.F., Leong, K.F., Du, Z.H., and Chua, C.K. The design of scaffolds for use in tissue engineering. Part 1. Traditional factors. *Tissue Eng* **7**, 679, 2001.

37. Asti, A., and Gioglio, L. Natural and synthetic biodegradable polymers: different scaffolds for cell expansion and tissue formation. *Int J Artif Organs* **37**, 187, 2014.
38. Pan, Z., and Ding, J. Poly(lactide-co-glycolide) porous scaffolds for tissue engineering and regenerative medicine. *Interface Focus* **2**, 366, 2012.
39. Li, W.-J., Laurencin, C.T., Caterson, E.J., Tuan, R.S., and Ko, F.K. Electrospun nanofibrous structure: a novel scaffold for tissue engineering. *J Biomed Mater Res* **60**, 613, 2002.
40. Kim, T.G., and Park, T.G. Biomimicking extracellular matrix: cell adhesive RGD peptide modified electrospun poly(D,L-lactic-co-glycolic acid) nanofiber mesh. *Tissue Eng* **12**, 221, 2006.
41. Subramanian, A., Krishnan, U.M., and Sethuraman, S. Fabrication of uniaxially aligned 3D electrospun scaffolds for neural regeneration. *Biomed Mater* **6**, 025004, 2011.
42. Cantara, S.I., Soscia, D.A., Sequeira, S.J., Jean-Gilles, R.P., Castracane, J., and Larsen, M. Selective functionalization of nanofiber scaffolds to regulate salivary gland epithelial cell proliferation and polarity. *Biomaterials* **33**, 8372, 2012.
43. Meng, Z.X., Li, H.F., Sun, Z.Z., Zheng, W., and Zheng, Y.F. Fabrication of mineralized electrospun PLGA and PLGA/gelatin nanofibers and their potential in bone tissue engineering. *Mater Sci Eng C* **33**, 699, 2013.
44. Prabhakaran, M.P., Mobarakeh, L.G., Kai, D., Karbalaie, K., Nasr-Esfahani, M.H., and Ramakrishna, S. Differentiation of embryonic stem cells to cardiomyocytes on electrospun nanofibrous substrates. *J Biomed Mater Res* **102**, 447, 2014.
45. Sterilization of health care products – General requirements for characterization of a sterilizing agent and the development, validation and routine control of a sterilization process for medical devices. ISO 14937:2009. Geneva, Switzerland: ISO, 2009.
46. Thanki, P.N., Dellacherie, E., and Six, J.-L. Surface characteristics of PLA and PLGA films. *Applied Surface Science*. **253**(5), 2758, 2006.

47. Lee, J.B., Kim, S.E., Heo, D.N., Kwon, I.K., and Choi, B.J. In vitro Characterization of Nanofibrous PLGA/Gelatin/Hydroxyapatite Composite for Bone Tissue Engineering. *Macromol Res* **18**, 1195, 2010.
48. Bailey, N.A., Sandor, M., Kreitz, M., and Mathiowitz, E. Comparison of the enthalpic relaxation of poly(lactide-co-glycolide) 50 : 50 nanospheres and raw polymer. *J Appl Polym Sci* **86**, 1868, 2002.
49. Park, J., and Kang, S. A Study on Surface, Thermal and Mechanical Properties of Absorbable PLGA Plate. *Int J Control Autom* **6**, 73, 2013.
50. Subramanian, A., Krishnan, U.M., and Sethuraman, S. Fabrication, Characterization and In Vitro Evaluation of Aligned PLGA-PCL Nanofibers for Neural Regeneration. *Ann Biomed Eng* **40**, 2098, 2012.
51. Selim, M., Bullock, A.J., Blackwood, K.A., Chapple, C.R., and MacNeil, S. Developing biodegradable scaffolds for tissue engineering of the urethra. *BJU Int* **107**, 296, 2011.
52. Sefat, F., McKean, R., Deshpande, P., Ramachandran, C., Hill, C.J., Sangwan, V.S., *et al.* Production, sterilisation and storage of biodegradable electrospun PLGA membranes for delivery of limbal stem cells to the cornea. *Procedia Eng* **59**, 101, 2013.
53. Dufresne, S., Leblond, H., and Chaunet, M. Relationship between lumen diameter and length sterilized in the 125L ozone sterilizer. *Am J Infect Control* **36**, 291, 2008.
54. World Health Organization. *The International Pharmacopoeia*, 4th ed. Geneva, Switzerland: World Health Organization, 2014. Available from URL: <http://apps.who.int/phint/en/p/about/>
55. Lee, J-J., Ho, M-H., and Hsiao, S-W. Immobilization of peptides by ozone activation to promote the osteoconductivity of PLLA substrates. *J Biomater Sci Polym Ed* **19**, 1637, 2008.

56. Montanari, L., Costantini, M., Signoretti, E.C., Valvo, L., Santucci, M., Bartolomei, M., *et al.* Gamma irradiation effects on poly(DL-lactide-co-glycolide) microspheres. *J Control Release* **56**, 219, 1998.
57. Rouse, J.J., Mohamed, F., and van der Walle, C.F. Physical ageing and thermal analysis of PLGA microspheres encapsulating protein or DNA. *Int J Pharm* **339**, 112, 2007.
58. Loo, J.S.C., Ooi, C.P., Boey, F.Y.C. Degradation of poly(lactide-co-glycolide) (PLGA) and poly(L-lactide) (PLLA) by electron beam radiation. *Biomaterials* **26**, 1359, 2005.
59. Loo, S.C.J., Ooi, C.P., and Boey, Y.C.F. Radiation effects on poly(lactide-co-glycolide) (PLGA) and poly(L-lactide) (PLLA). *Polym Degrad Stabil* **83**, 259, 2004.
60. Full, S.M., Delman, C., Gluck, J.M., AbDMAulen, R., Shemin, R.J., and Heydarkhan-Hagvall, S. Effect of fiber orientation of collagen-based electrospun meshes on human fibroblasts for ligament tissue engineering applications. *J Biomed Mater Res Part B Appl. Biomater* **103**, 39, 2015.
61. Jia, L., Prabhakaran, M.P., Qin, X., and Ramakrishna, S. Guiding the orientation of smooth muscle cells on random and aligned polyurethane/collagen nanofibers. *J Biomater Appl* **29**, 364, 2014.

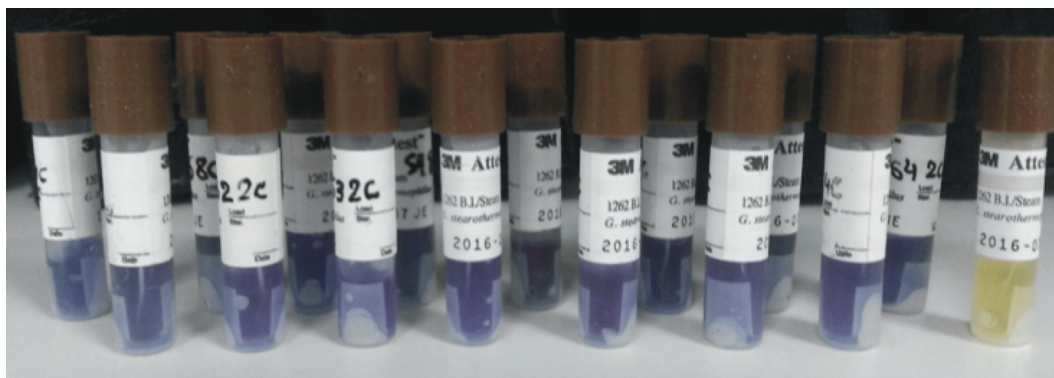


Figure 1. Fifteen ozone gas-sterilized *G. stearotherophilus* indicators (purple) compared to a non-sterilized one (yellow) after 48 hours incubation at 56 °C.

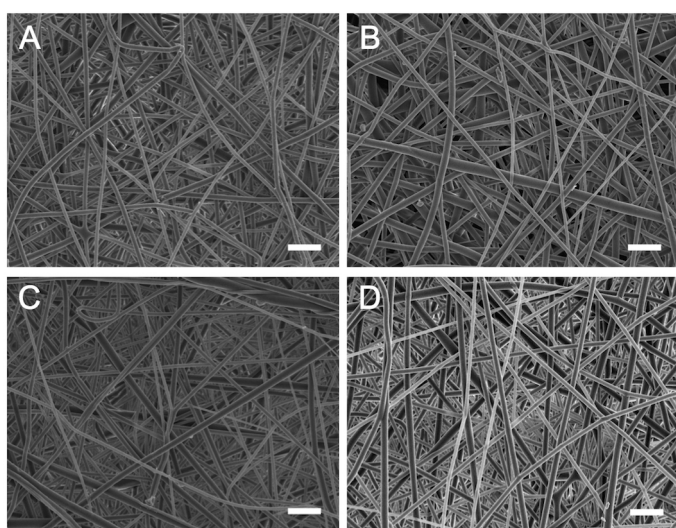


Figure 2. FE-SEM micrographs of (A) non-sterilized and sterilized PLGA nanofibre scaffolds after (B) 2, (C) 4, and (D) 8 pulses of ozone gas. Scale bars = 5 µm.

Table 1. Summary of morphology, surface and bulk properties of non-sterilized and ozone gas sterilized PLGA scaffolds (n=3).

Ozone Sterilization	Fibre Diameter (nm)	Contact angle (°)	ΔH_{relax} (J/g)*	T_g (°C)**	Tensile Strength (MPa)	Young's Modulus (MPa)
None	670 ± 40	128.3 ± 1.3	8.8 ± 0.4	51.8 ± 0.1	3.41 ± 0.11	118 ± 5
2 pulses	634 ± 36	125.6 ± 0.4	9.8 ± 0.2	51.8 ± 0.1	3.75 ± 0.14	128 ± 6
4 pulses	636 ± 51	126.1 ± 0.6	9.7 ± 0.2	52.0 ± 0.1	3.33 ± 0.18	114 ± 7
8 pulses	664 ± 28	124.5 ± 0.7	9.7 ± 0.2	51.6 ± 0.1	2.91 ± 0.15	88 ± 3

* Enthalpy Relaxation (first scan)

** Glass transition temperature obtained from the second scan

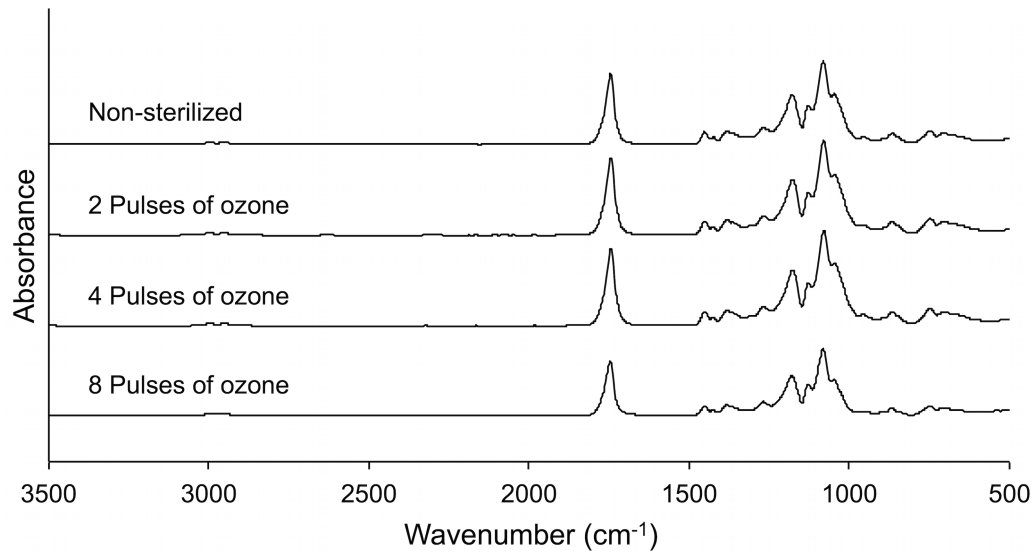


Figure 3. ATR-FTIR spectra of electrospun PLGA nanofibres prior to sterilization, and after 2, 4 or 8 pulses of ozone gas.

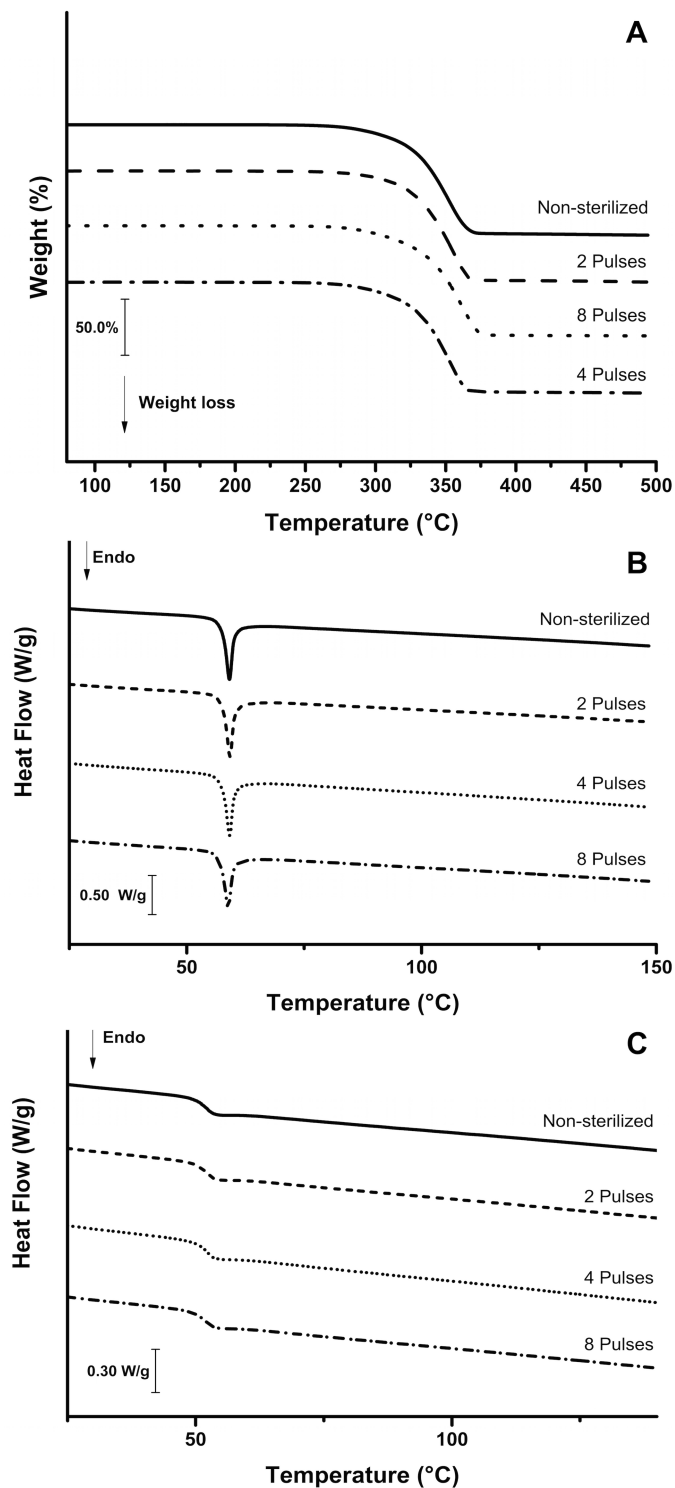


Figure 4. Thermoanalytical characterisation of non-sterilized and sterilized PLGA scaffolds. (A) Thermogravimetric curves obtained in a dynamic argon atmosphere (100 mL/min) and heating rate 10 °C/min; (B) DSC curves obtained in a dynamic argon atmosphere (50 mL/min) and heating rate 10 °C/min; (C) DSC curves with pronounced glass transition events obtained in a second scan (thermal treatment) under a dynamic argon atmosphere (50 mL/min) and heating rate 10 °C/min.

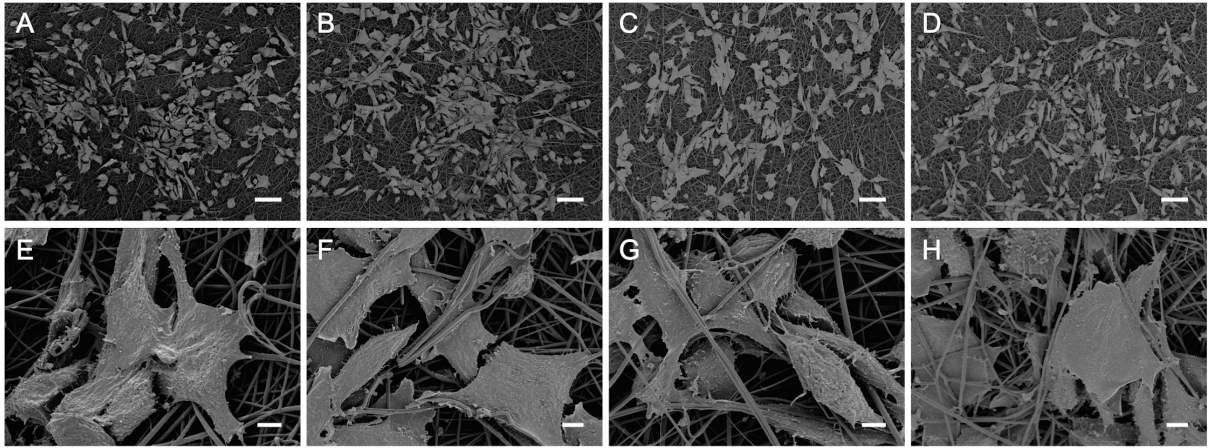


Figure 5. Interaction and spreading of 3T3 fibroblasts on PLGA nanofibre scaffolds 24 hours after cell seeding: (A, E) non-sterilized mat; (B, F) sterilized by 2 pulses of ozonation; (C, G) sterilized by 4 pulses of ozonation; (D, H) sterilized by 8 pulses of ozonation. Scale bars = 50 μm (A-D) and 5 μm (E-H).

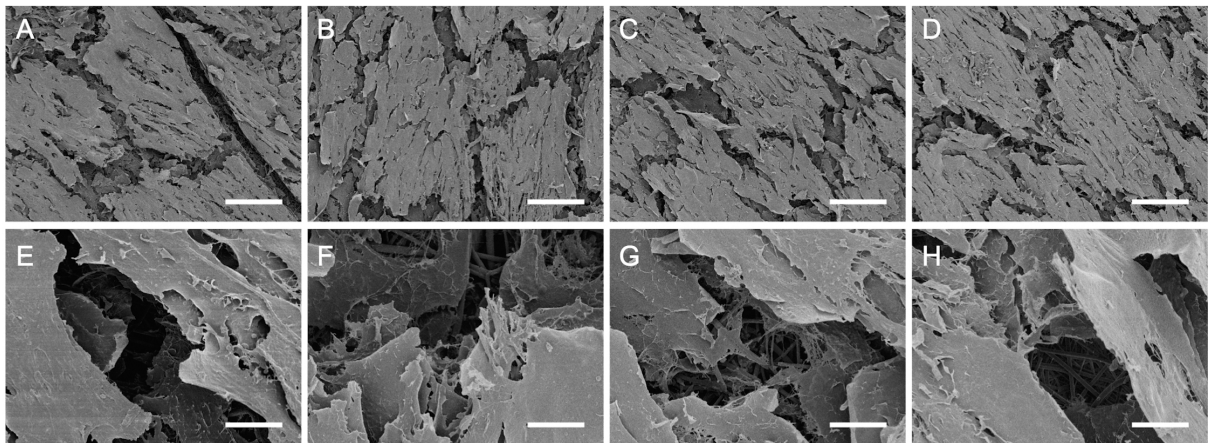


Figure 6. 3T3 fibroblasts on PLGA nanofibre scaffolds 15 days after seeding: (A, E) non-sterilized mat; (B, F) sterilized by 2 pulses of ozonation; (C, G) sterilized by 4 pulses of ozonation; (D, H) sterilized by 8 pulses of ozonation. Scale bars = 100 μm (A-D) and 10 μm (E-H).

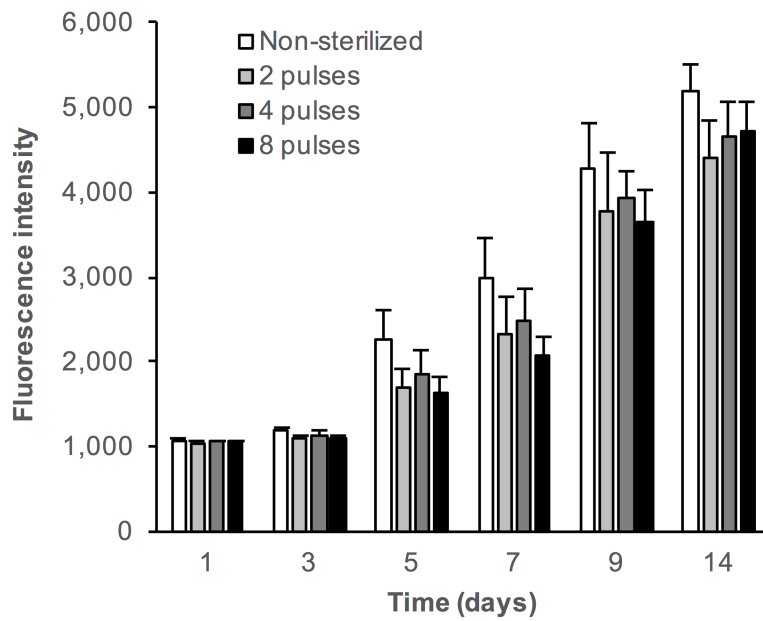


Figure 7. 3T3 fibroblast proliferation on non-sterilized and ozone gas-sterilized PLGA nanofibre scaffolds determined by the reduction of resazurin to resorufin. Data represent the mean + standard error (n=3).